

1 INTRODUCTION

The Tevatron started its operation again in collider mode in summer 2001. In the first phase, termed Run IIa, 36 \bar{p} bunches in three trains of twelve bunches collide with 36 proton bunches, see Figure 1. This is a six-fold increase in

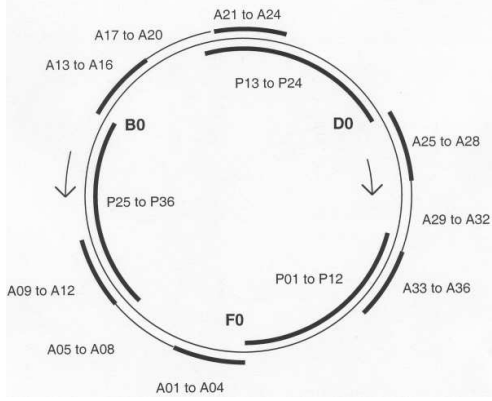


Figure 1: Beam spacing and injection configuration. The proton and antiproton bunches are labeled P01, P02, ... and A01, A02, ... starting from the upstream end of the bunch train so that A01 and P01 meet at F0.

the number of bunches from the last collider operation Run Ib. Table 1 shows the main beam parameters. Design proton intensities are higher so the head-on beam-beam tune shifts experienced by the anti-protons will be higher than in Run Ib. The greater number of long-range beam-beam interactions will increase the total beam-beam induced tune spread of the anti-protons. Furthermore these effects are different for each \bar{p} bunch in a train since the sequence of long-range interactions is different for each of them. For

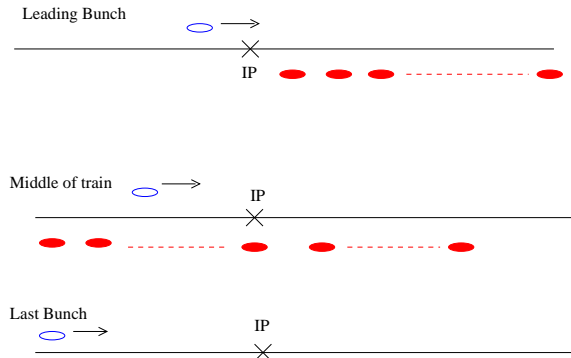


Figure 2: Bunch 1, 6 and 12 in a train crossing at IP

example in Figure 2 the leading bunch 1 will experience all long-range interactions downstream of the IP, middle bunch 6 will experience five interactions upstream and six interactions downstream of the IP while the trailing bunch 12 will experience all long-range interactions upstream of the IP. All of these effects taken together may reduce the dynamic aperture (DA) and/or lifetime of the anti-protons significantly. In the second stage of Run II, named RUN IIb,

the plan is to increase the luminosity further with more intense bunches, larger number of bunches (140X103) to decrease the number of interactions per bunch crossing, and also introduce crossing angles at B0 and D0 to avoid parasitic collisions with zero separation.

Table 1: Main beam parameters in Run I and Run II

	Run Ib	Run IIa
	p/\bar{p}	p/\bar{p}
Luminosity [$\text{cm}^{-2}\text{sec}^{-1}$]	1.6×10^{31}	8.6×10^{31}
Bunch Intensities $\times 10^{11}$	(2.3/0.55)	(2.7/0.3)
Emittances 95% [mm-mrad]	23/13	20/15
Number of bunches	6	36
Bunch separation [m]	1049.3	118.8
Beam size at IP [μm]	37/28	33/29
Beam-beam parameter ξ/IP $\times 10^{-3}$	3.4/7.4	1.5/9.9

2 BEAM-BEAM INTERACTIONS IN RUN IIa

In Run IIa each bunch will experience two head-on interactions at B0 and D0 and seventy long-range interactions. These long-range interactions will be distributed over the entire ring with differing beam separations and differing phase advances from one interaction to the next. Figure 3 shows the beam separation (in units of the rms bunch size) at all the seventy two locations of beam-beam interactions for bunch 6. At most locations the beam separation is of the order of 10σ . The prominent exceptions are the parasitic collisions nearest to the IPs where the separation is only about 6σ . These nearest interactions in fact also have the dominant contribution to the tune footprint. The strength of each beam-beam kick and the phase ad-

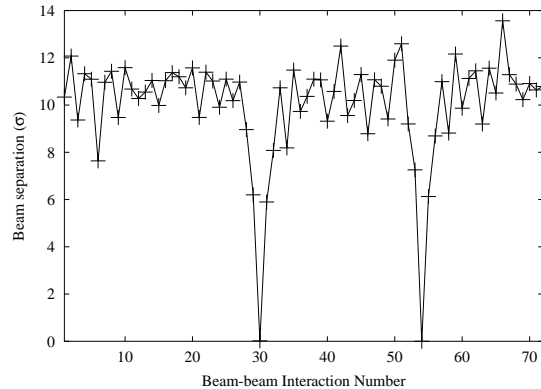


Figure 3: Separation between \bar{p} bunch 6 and the opposing proton bunch at all 72 beam-beam interactions. The head-on collisions are at locations 30(D0) and 54(B0).

vanance between kicks are important parameters. One way to parametrize the strength of a kick with separated beams is

by the tune shift experienced by zero amplitude particles. This is similar to the convention of using the beam-beam parameter ξ to parametrize the strength of head-on beam-beam collisions. For beams with arbitrary aspect ratios, the tune shifts of a particle at zero amplitude can be calculated analytically. The results show that there is a significant dependence of the tune shift on the angle between the weak and strong beams for each aspect ratio, hinting to the possibility of tune shift compensation schemes by choosing the right orientation in the separation plane for each aspect ratio, concomitant with constant separation.

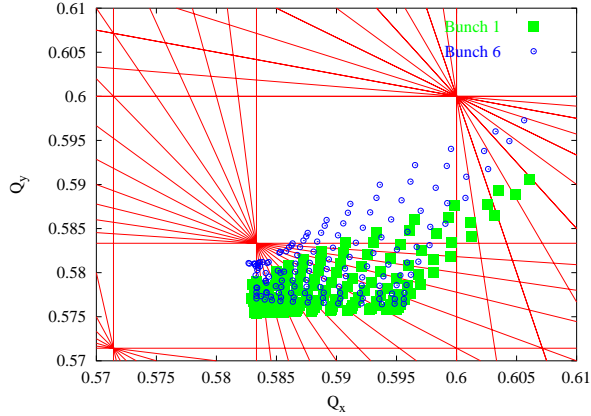


Figure 4: Tune footprint for bunches 1 and 6 in a train.

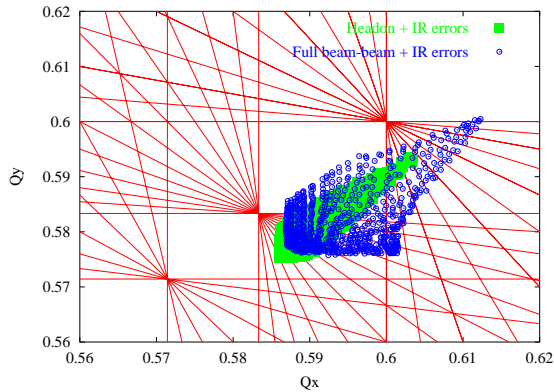


Figure 5: Tune footprint of \bar{p} bunch 6 with (i) the head-on interactions and (ii) all the beam-beam interactions. IR errors and chromaticity sextupoles are included in each case. The footprint is shown for particles with amplitudes up to 7σ . Nearby fifth, seventh, tenth and twelfth order sum resonances are shown. The linear lattice tune is $(0.585, 0.575)$.

Sometimes the footprint is a good measure of the strength of the nonlinearities. Figure 4 shows the footprints due to the beam-beam interactions in Run IIa for bunch 1 and bunch 6 superposed on nearby sum resonances up to twelfth order. Footprints of all bunches except for bunch 1 and 12 are clustered around that of bunch 6. The major differences in the tunes between bunch 6 and bunch 1 and 12 are due to the missing parasitic collision closest

to the IP, upstream for bunch 1 and downstream for bunch 12. The variation in the tune shift and in the tune spread from bunch to bunch will be greatly enhanced in Run IIb when the number of bunches is increased to more than one hundred. The Tevatron beam-beam compensation project [1] aims to reduce this spread in tunes by colliding anti-proton bunches with a low energy electron beam whose intensity will be varied from bunch to bunch. However even in Run IIa, the stronger beam-beam interactions at the IP ($\xi \approx 0.01$ compared to $\xi \approx 0.0074$ in Run Ib) and the larger number of long-range interactions may cause emittance growth and reduced lifetime of the anti-protons. The tune footprint shown in Figure 5 is for \bar{p} bunch 6 in two cases. We can see the addition of the long-range interactions increases the tune spread significantly and particles at amplitudes up to approximately 3σ now straddle the 5th and 10th order resonances. The nominal working point ($\nu_x = 0.585, \nu_y = 0.575$) is chosen to lie between fifth and seventh order resonances. At this working point the Tevatron beam straddles twelfth order sum resonances. Operational experience during Run I showed that these resonances did not cause a significant reduction in lifetime. However the tune footprints and nonlinearities were also smaller in Run I. Inclusion of the IR errors does not change the footprint significantly.

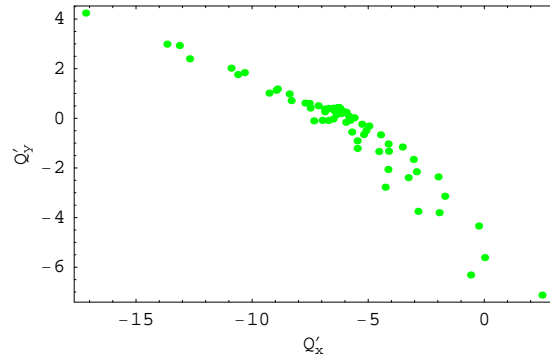


Figure 6: The analytically computed linear chromaticity footprint with all beam beam interactions included for particles with amplitudes up to 6σ .

Synchrotron oscillations introduce new dynamical issues at Tevatron. The bunch length in the Tevatron is comparable to the beta function at the IP, $\sigma_s \approx 37$ cm, $\beta^* = 35$ cm. In this case, the head-on beam-beam force is modulated by the longitudinal position of the particle. Strengths of transverse betatron resonances depend on the synchrotron amplitude and in addition synchrotron sideband resonances are created around each betatron resonance. Synchro-betatron resonances are also created when the chromaticity is non-zero. Beam stability requires that the linear chromaticity be corrected to a value near +5 at top energy. The long-range beam-beam force in the Tevatron creates an additional amplitude dependent chromaticity[2]. The source of this chromaticity is the horizontal and vertical dispersion at the parasitic collisions which makes the beam separation depend on

3 DYNAMIC APERTURE CALCULATIONS

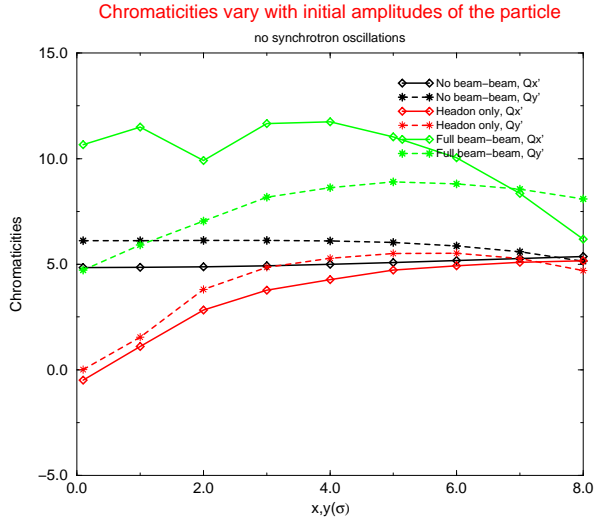


Figure 7: Variation of chromaticities with particle amplitude in pbar bunch 6, evaluated along the diagonal in coordinate space, computed by tracking.

the momentum deviation $\Delta p/p$. Figure 6 gives the analytically computed linear chromaticity footprint with all beam beam interactions included, while Figure 7 gives the amplitude dependent chromaticity, evaluated along the diagonal in coordinate space, computed by tracking in a variety of scenarios.

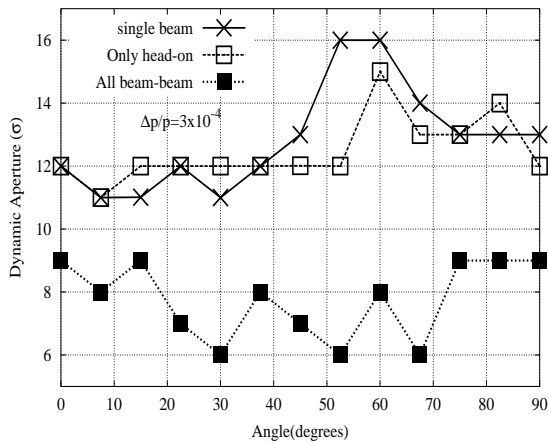


Figure 8: 6D dynamic aperture of pbar bunch 6 after 100,000 turns (about 72 synchrotron periods) as a function of angle in transverse coordinate space for three cases: (1) single beam, (2) machine nonlinearities and only the head-on beam-beam interactions and (3) machine nonlinearities and all beam-beam interactions.

The simulation model includes the beam-beam kicks, the nonlinear fields in the Interaction Region (IR) quadrupoles (the beta functions in these magnets is about an order of magnitude greater than the values in the arcs) and the chromaticity correcting sextupoles. The bunch length effects [3], which include hour glass effects and phase averaging, were taken into account in the simulations of the head-on interactions described below. The long-range effects are modelled by delta function kicks.

Mostly simulations were done by code MAD. In this report linear imperfections such as orbit errors and coupling due to misalignments are not included and neither are time-dependent effects such as those due to power supply ripple. Synchrotron oscillations and other momentum dependent effects have yet to be studied in sufficient detail. These effects are important and will be included in further studies.

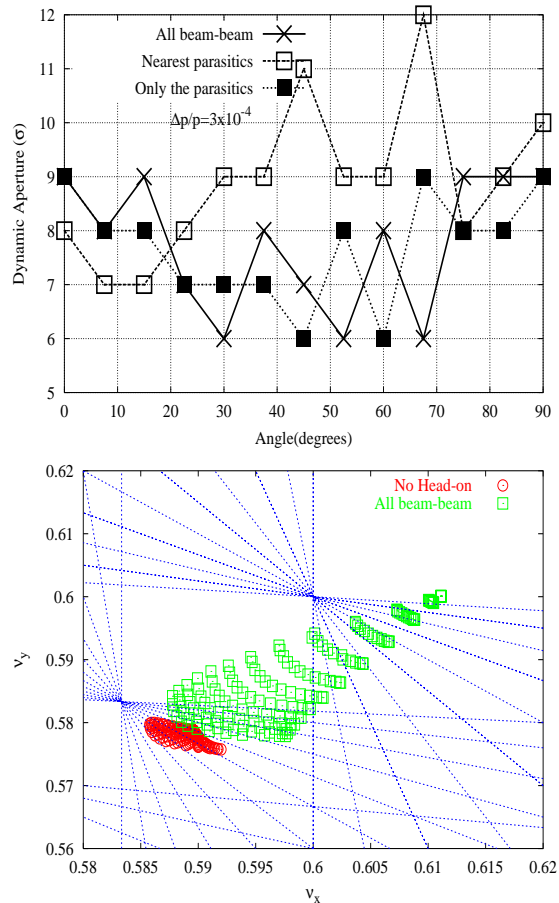


Figure 9: Upper: 6D dynamic aperture of pbar bunch 6 after 100,000 turns for three cases: (1) all beam-beam interactions, (2) head-on and nearest parasitics and (3) only the parasitics. Lower: Footprint of anti-proton bunch 6 with (i) all parasitic interactions but no head-on and (ii) all the beam-beam interactions.

Figure 8 shows the 6D dynamic aperture for three different cases. The upper plot of Figure 9 shows the 6D dynamic aperture vs angle for the special but unphysical cases where all the parasitic interactions are included but the head-on collisions are not. The footprint for this case is also shown in the lower plot of Figure 9. We can see the footprint is considerably smaller and does not cross any resonance of order lower than the twelfth. However, the dynamic aperture is nearly the same as with all the beam-beam interactions. It is evident that the stable region is determined by the parasitic interactions - they completely dominate the effects due to the head-on collisions.

The calculations of the dynamic aperture are summarized in Table 2. Figure 10 shows the survival plot for three cases: single beam, bunch 1 and bunch 6. In each case, the stable amplitude along the most unstable angle in coordinate space is shown. This survival plot is another representation of the fact that after 10^5 turns the stable region for the single beam does not change much while with beam-beam interactions, the stable region diminishes with time.

Bunch 6: $\nu_x = 0.585, \nu_y = 0.575$ DA after 10^5 turns, $\Delta p/p = 3 \times 10^{-4}$	
	$(\langle DA \rangle, DA_{min})$
IR errors	(12.9, 11.0)
Head-on and IR errors	(12.5, 11.0)
Head-on, nearest PCs, IR errors	(8.9, 7.0)
Head-on, nearest PCs at 10σ , IR errors	(10.2, 8.0)
Only the parasitics, IR errors	(7.7, 6.0)
All beam-beam, IR errors	(7.7, 6.0)
bunches 6 and 1 DA after 10^6 turns, $\Delta p/p = 3 \times 10^{-4}$	
Single beam	(12.3, 11.0)
Bunch 6: all beam-beam	(5.4, 4.0)
Bunch 1: all beam-beam	(5.6, 3.0)

Table 2: The average and minimum 6D dynamic aperture with various configurations of beam-beam interactions. Note that the dynamic aperture with only the parasitics is nearly the same as that with all the beam-beam interactions. The head-on interactions therefore are dominated by the parasitics. Also shown are the average and minimum 6D dynamic aperture for bunches 1 at the edges of the bunch train compared with bunch 6 in the middle of the train.

4 CONCLUSIONS

- At design parameters and after 10^6 turns, the DA for bunch 6 is about 5σ (6D, $\Delta p/p = 3 \times 10^{-4}$, $\nu'_x = \nu'_y = 5$). This value is smaller than the aperture limitation set by the primary collimators (8σ)
- A tune scan around the nominal working point showed that the DA does not change significantly as long as the tunes are sufficiently far from the 5th and 7th order resonances.

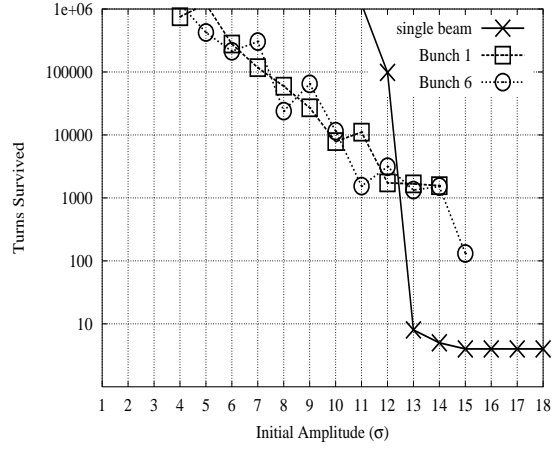


Figure 10: Survival plots for three cases along the most unstable angle in each case. In each case, particles were given a momentum deviation of $\Delta p/p = 3 \times 10^{-4}$. For the single beam, the stable region stabilizes after about 10^5 turns. With the beam-beam interactions, the stable area appears to progressively diminish with time.

- The tune footprint is largely determined by the head-on interactions. However they have very little influence on the dynamic aperture. Hence it is not obvious that compressing the footprint would improve the dynamic aperture. Of the seventy long-range interactions the four interactions nearest to the two IPs are the dominant group.
- With a tune scan and 4D tracking we find that at amplitudes of 6σ and 7σ the seventh order sum resonances, particularly the $4\nu_x + 3\nu_y$ and $5\nu_x + 2\nu_y$ resonances, cause large amplitude growth within 10^3 turns.
The synchro-betatron resonances at the nominal working point do not appear to be responsible for fast loss but the additional streaming channels created by the sideband resonances $m_x\nu_x + m_y\nu_y + m_s\nu_s = p$ of the twelfth order sum resonances, in particular $(m_x, m_y) = (3, 9), (4, 8), (7, 5), (8, 4)$ and $|m_s| \leq 3$, destabilize particles that would be stable without synchrotron oscillations over longer time scales.
- The differences in DA between these two bunches are not significant but bunch 1 may have a marginally smaller DA.

5 REFERENCES

- [1] V. Shiltsev, <http://www-ap.fnl.gov/meiqin/beambeam01/beambeam01.html>
- [2] Y. Alexahin, <http://www-ap.fnl.gov/meiqin/beambeam01/beambeam01.html>
- [3] T. Sen, Fermilab preprint, to be published